Supporting Information

Exploitation of Two-Dimensional Conjugated Covalent Organic Frameworks Based on Tetraphenylethylene with Bicarbazole and Pyrene Units and Applications in Perovskite Solar Cells

Mohamed Gamal Mohamed,[a+] Chia-Chen Lee,[b,c+] Ahmed F. M. EL-Mahdy,[a+] Johann Lüder,[a,d] Ming-Hsuan Yu,[b] Zhen Li,[c] Zonglong Zhu,[c] Chu-Chen Chueh,[b,e] and Shiao-Wei Kuo[a,f*]*

[a] Prof. M. G. Mohamed, Prof. A. F. M. EL-Mahdy, Prof. J. Lüder, and Prof. S.-W. Kuo
Department of Materials and Optoelectronic Science and Center of Crystal Research, National Sun Yat-Sen University, Kaohsiung 80424, Taiwan

[b] C.-C. Lee and Prof. C.-C. Chueh
Department of Chemical Engineering, National Taiwan University, Taipei 10617, Taiwan.

[c] C.-C. Lee, Z. Li, and Prof. Z. Zhu
Department of Chemistry, City University of Hong Kong, Kowloon 999077, Hong Kong.

[d] Prof. J. Lüder
Department of Materials and Optoelectronic Science, National Sun Yat-Sen University, Kaohsiung 80424, Taiwan

[e] Prof. C.-C. Chueh
Advanced Research Center for Green Materials Science and Technology, National Taiwan University, Taipei 10617, Taiwan.

[f] Prof. S.-W. Kuo
Department of Medicinal and Applied Chemistry, Kaohsiung Medical University, Kaohsiung, Taiwan.

[+] These authors are equally contributed to this work.

*Corresponding author. E-mail: cchueh@ntu.edu.tw; kuosw@faculty.nsysu.edu.tw

Keywords: Covalent organic frameworks; perovskite solar cells; interfacial materials

➢ S1. Synthetic Procedures

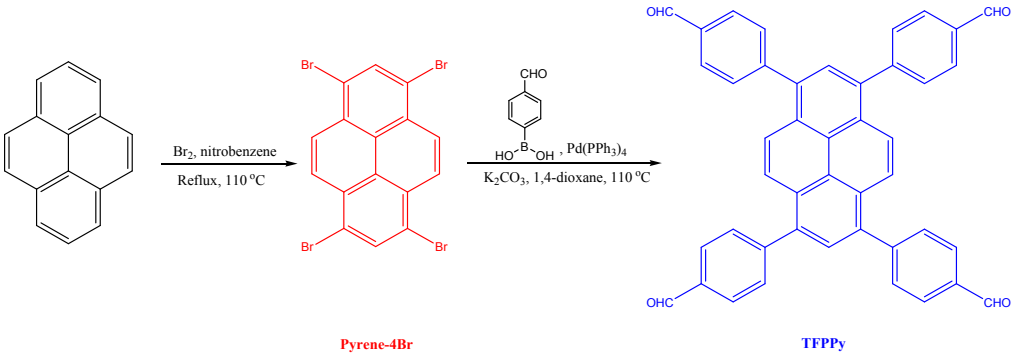

Scheme S1. Synthesis of 1,3,6,8-Tetra(4-formylphenyl)pyrene (TFPPy).

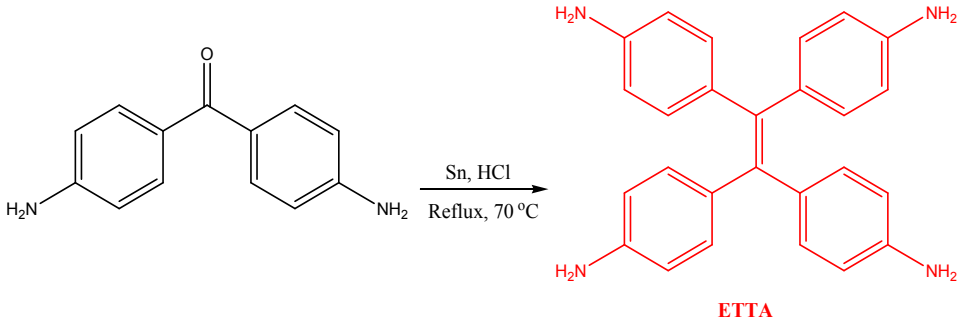

Scheme S2. Synthesis of 4,4',4",4"'-(ethane-1,1,2,2-tetrayl)tetranilino (ETTA).

Synthesis of 4,4',4",4"'-(ethane-1,1,2,2-tetrayl)tetranilino (ETTA)[S2]

In a 250 mL two neck-bottle, 4,4'-diaminobenzophenone (1.00 g, 4.50 mmol) was dissolved in 45 mL of hydrochloric acid (37%) at 60 °C with stirring under N_2. Then, tin powder (3.00 g, 25 mmol) was added to the reaction mixture, and the reaction mixture was heated at 75 °C for 18 h. After cooling, the precipitate was filtrated and washed with sodium hydroxide (1N), water and methanol and dried under vacuum at 50 °C for 24 h to afford ETTA as a green powder 1.35 g. FT-IR (cm^{-1}): 3358, 3420, 3025, 1620, 1520. ^{1}H-NMR (DMSO-d_6, 25 °C, 500 MHz): δ = 6.59 (d, J = 8.72 Hz, 8H), 6.27 (d, J = 8.36 Hz, 8H), 4.85 (s, 8H). ^{13}C-NMR (DMSO-d_6, 25 °C, 500 MHz): δ = 146.0 (C), 136.6(C), 132.9 (C), 131.6 (CH), 113.1 (CH).

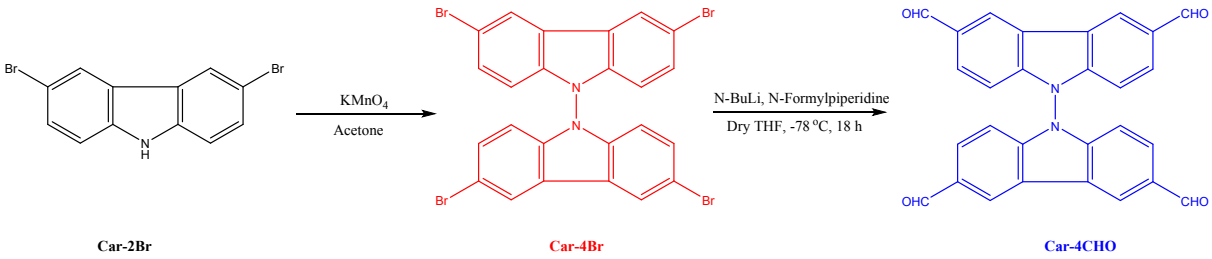

Scheme S3. Synthesis of 3,3',6,6'-tetraformyl-9,9'-bicarbazole (Car-4CHO).

Synthesis of 3,6-dibromocarbazole (Car-2Br)[S3]

In a 500 mL two neck-bottle, A solution of N-bromosuccinimide NBS (5.00 g, 28 mmol) in 25 mL of dry DMF was added dropwise for 1 h to a suspension of carbazole (2.34 g, 14 mmol) in dichloromethane (140 mL). Then, the reaction mixture was stirred at room temperature for 24, and the reaction mixture was extracted three times by H_2O, and the organic layer was dried under anhydrous magnesium sulfate ($MgSO_4$) and filtered. Then, DCM was evaporated by rotatory evaporator and the residue was dissolved in acetone (25 mL) and precipitated with hexane (150 mL). The solid was filtrated and dried under vacuum at 50 °C to afford 3,6-dibromocarbazole as white solid (3.6 g). ^{1}H-NMR ($CDCl_3$, 25 °C, 500 MHz): δ = 7.31 (d, *J* = 8.6 Hz, 2H), 7.52 (d, *J* = 8.6 Hz, 2 H), 8.13 (d, *J* = 1.9 Hz, 2H), and 10.37 (s, 1 H). ^{13}C-NMR ($CDCl_3$, 25 °C, 125 MHz): δ = 139.40, 129.26, 124.45, 113.07, 112.32.

Synthesis of 3,3',6,6'-tetrabromo-9,9'-bicarbazole (Car-4Br)[S3]

1n a 250 mL one neck-bottle, 3,6-dibromocarbazole (3.00 g, 9.23 mmol), potassium permanganate (4.38 g, 27.92 mmol) was dissolved in 50 mL acetone and heated at 50 °C for 4 h. Then the reaction mixture was hydrolyzed with 50 mL distilled water. The reaction mixture was extracted with three times by dichloromethane (DCM) and the organic layer was dried over anhydrous $MgSO_4$ and concentrated under reduced pressure to obtain Car-4Br

as a white powder (6.92 g). ^{1}H-NMR ($CDCl_3$, 25 ^{o}C, 500 MHz): δ = 8.26 (d, 4 H), 7.47 (d, *J* = 10.4 Hz, 4H), 6.74 (d, *J* = 8.6 Hz, 4H). ^{13}C-NMR ($CDCl_3$, 25 ^{o}C, 125 MHz): δ = 139.34, 131.26, 124.49, 123.14, 115.56, 110.82.

Synthesis of 3,3',6,6'-tetraformyl-9,9'-bicarbazole (Car-4CHO)[S3]

1n a 250 mL three neck-bottle n-Butyl lithium (2.4 M, 8.7 mL, 20 mmol) was dropwise added to a solution of 3,3',6,6'-tetraformyl-9,9'-bicarbazole (1.296 g, 2.0 mmol) in 200 mL THF at -78 °C under N_2 atmosphere. The reaction mixture was stirred at the same temperature (-78 ^{o}C) for 2 h. After that, 2.5 mL of N-formylpipridine was dropwise added to the reaction mixture. Then, the reaction mixture was stirred for 24 h, followed by hydrolyzed with 50 mL HCl. Then, THF solution was removed by a rotatory evaporator to give a white solid (0.30 g). FT-IR (cm^{-1}): 2842, 2752, 1695, 1595. ^{1}H-NMR ($CDCl_3$, 25 ^{o}C, 500 MHz): δ = 10.20 (s, 4 H), 8.86 (s, 4 H), 8.02 (d, *J* = 9.6 Hz, 4 H), 7.08 (d, *J* = 8.4 Hz, 4 H). ^{13}C-NMR ($CDCl_3$, 25 ^{o}C, 125 MHz): δ = 190.95, 143.26, 132.24, 129.54, 124.17, 122.41, 109.61.

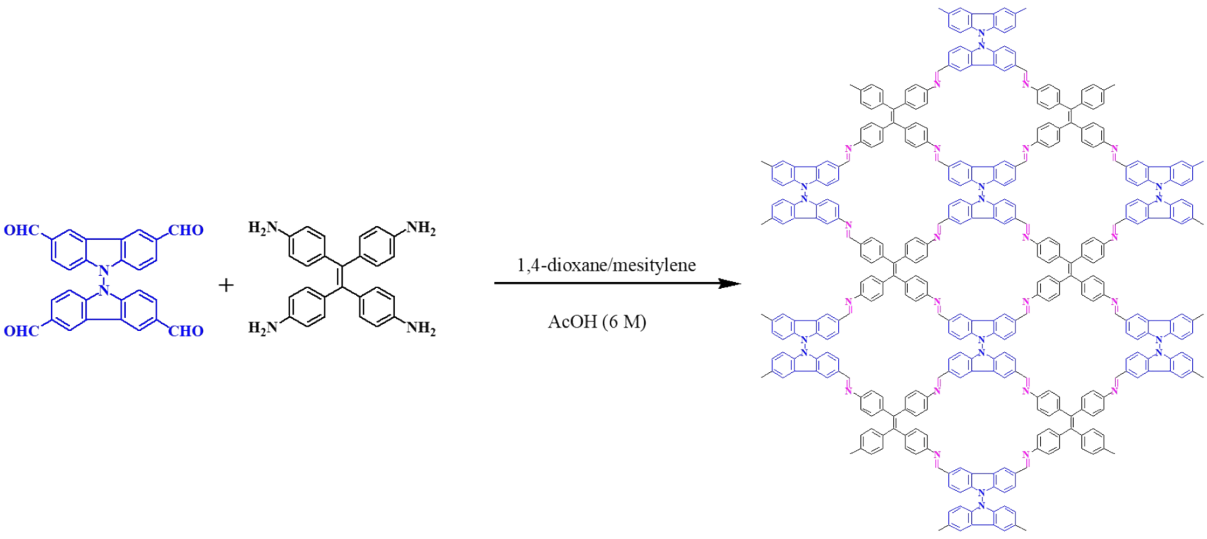

Scheme S4. Synthesis of Car-ETTA COF.

Synthesis of Car-ETTA COF

In a 25 mL Pyrex tube, ETTA (87.00 mg, 0.22 mmol) and Car-4CHO (100 mg, 0.23 mmol) was dissolved into 1,4-dioxane/mesitylene (5 mL/5 mL) mixture in the presence of acetic acid (6M, 1.00 mL). The tube was then sealed and degassed by three freeze-pump-thaw cycles. The tube was sealed off by flame and heated at 120 °C for 3 days. After cooling to room temperature, the tube was opened and the yellow precipitate was filtered and washed three times with NMP, THF, methanol and acetone respectively. The solid was dried under vacuum at 120 °C overnight to afford Car-ETTA COF as a yellow powder.

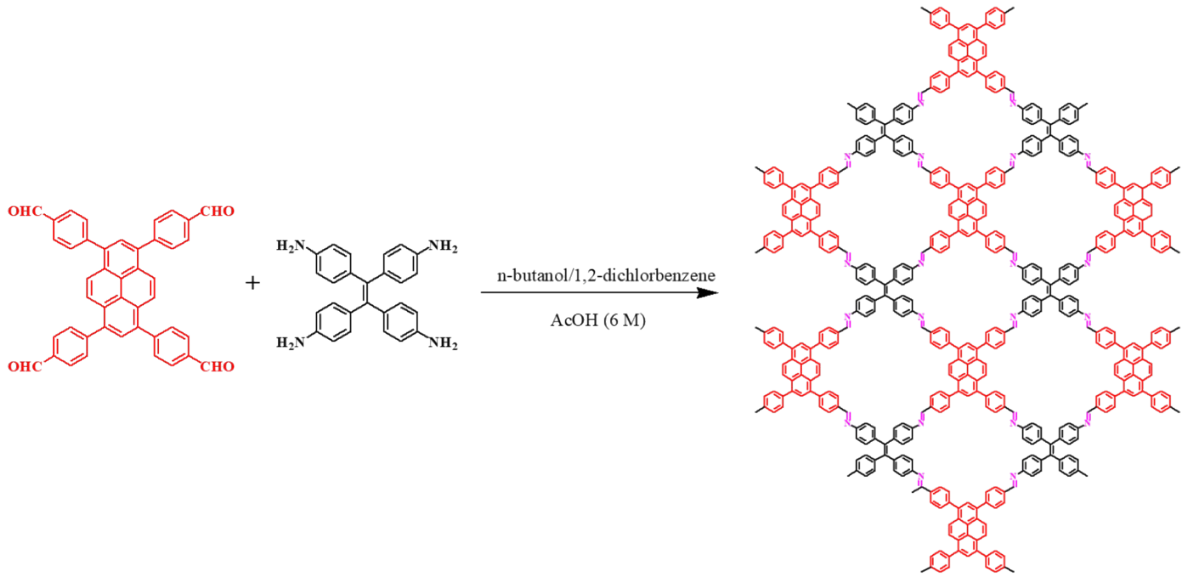

Scheme S5. Synthesis of TFPPy-ETTACOF.

Synthesis of TFPPy-ETTA COF

In a 25 mL Pyrex tube, ETTA (63.00 mg, 0.16 mmol) and TFPPy (100 mg, 0.16 mmol) was dissolved into n-butanol/1,2-dichlorobenzene (5 mL/5 mL) mixture in the presence of acetic acid (6M, 1.00 mL). The tube was then sealed and degassed by three freeze-pump-thaw cycles. The tube was sealed off by flame and heated at 120 °C for 3 days. After cooling to room temperature, the tube was opened and the yellow precipitate was filtered and washed three times with NMP, THF, methanol and acetone respectively. The solid was dried under vacuum at 120 °C overnight to afford TFPPy-ETTA COF as a yellow powder.

➢ S2. Characterization

Proton and carbon nuclear magnetic resonance (^{1}H and ^{13}C NMR) spectra were recorded using an INOVA 500 instrument with DMSO-d_6 and $CDCl_3$ as solvents and tetramethylsilane (TMS) as the external standard. Chemical shifts are provided in parts per million (ppm). Fourier transform mass spectra (electrospray ionization, ESI) of were recorded using a Bruker Solarix spectrometer. FTIR spectra were recorded using a Bruker Tensor 27 FTIR spectrophotometer and the conventional KBr plate method; 32 scans were collected at a resolution of 4 cm^{-1}. Solid state nuclear magnetic resonance (NMR) spectra were recorded using a Bruker Avance 400 NMR spectrometer and a Bruker magic angle spinning (MAS) probe, running 32,000 scans. Cross-polarization with MAS (CP/MAS) was used to acquire ^{13}C NMR spectral data at 75.5 MHz. The CP contact time was 2 ms; ^{1}H decoupling was applied during data acquisition. The decoupling frequency corresponded to 32 kHz. The MAS sample spinning rate was 10 kHz. Powder X-ray diffraction (PXRD) was carried out with a Siemens D5000 using monochromated Cu/Kα (λ = 0.1542 nm). The sample was spread in a thin layer on the square recess of an XRD sample holder. Field emission scanning electron microscopy (FE-SEM) was conducted using a JEOL JSM-7610F scanning electron microscope. Samples were treated via Pt sputtering for 100 s prior to observation. Transmission electron microscope (TEM) images were obtained with a JEOL JEM-2010 instrument operated at 200 kV. BET surface area and porosimetry measurements of the prepared samples (ca. 40-100 mg) were performed using a Micromeritics ASAP 2020 Surface Area and Porosity analyzer. Nitrogen isotherms were generated through incremental exposure to ultrahigh-purity N_2 (up to ca. 1 atm) in a liquid nitrogen (77 K) bath. Surface parameters were determined using BET adsorption models in the instrument's software. TGA was performed using a TA Q-50 analyzer under a flow of N_2 atmosphere. The samples were sealed in a Pt cell and heated from 40 to 800 °C at a heating rate of 20 °C min^{-1} under a flow of N_2 atmosphere at a flow rate of 60 mL min^{-1}. Molecular

modeling was performed using Reflex, a software package for crystal determination from XRD patterns, implemented in MS modeling (v. 4.4, Accelrys). Unit cell dimensions were first manually determined from the observed XRD peak positions using the coordinates.

➢ S3. NMR Spectral Profiles of Monomers and COF

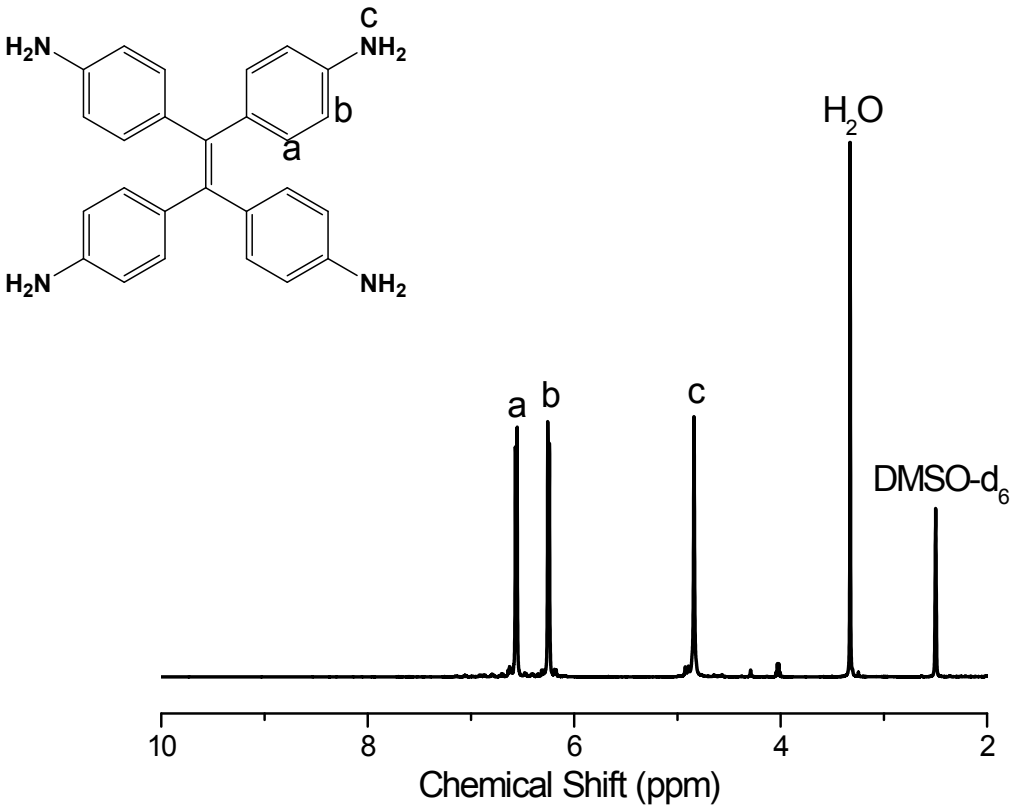

Figure S1. ^{1}H-NMR of ETTA in DMSO-d_6 as solvent.

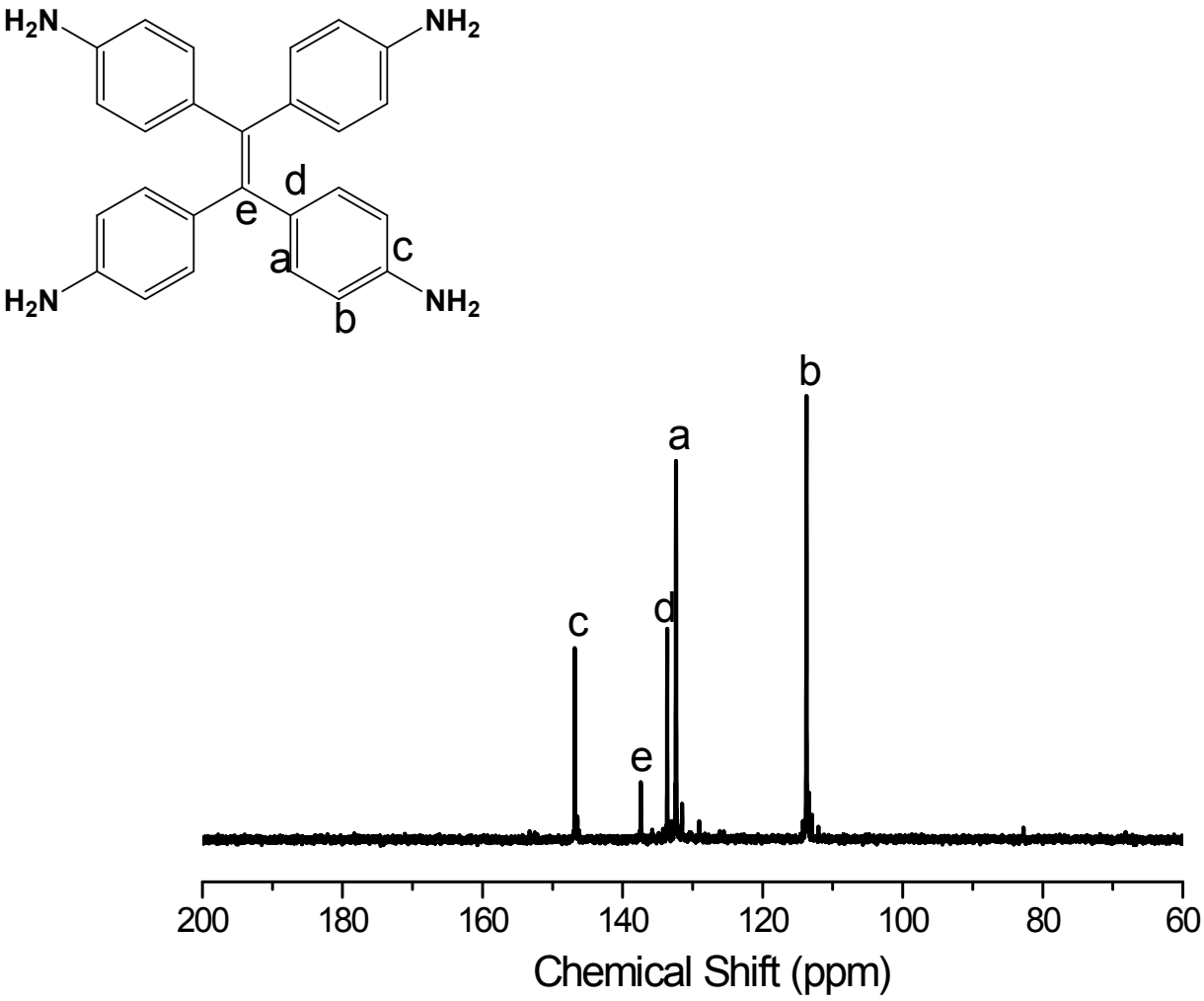

Figure S2. ^{13}C-NMR of ETTA in DMSO-d_6 as solvent.

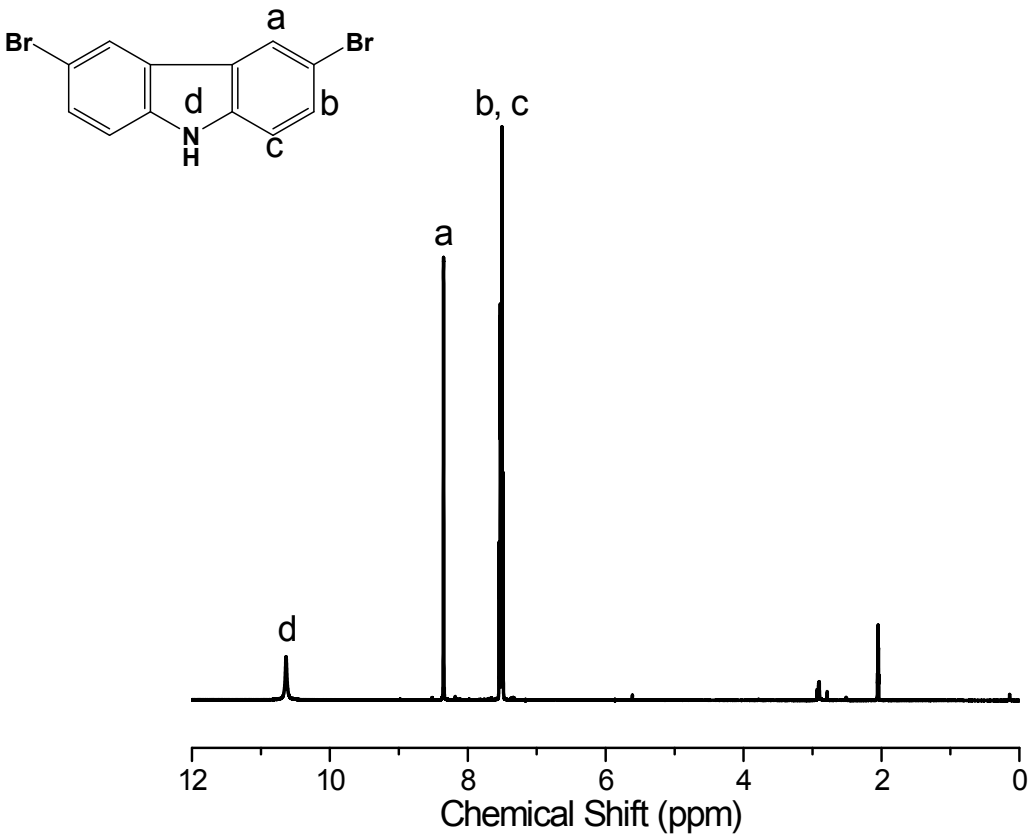

Figure S3. ^{1}H-NMR of Car-2Br in $CDCl_3$ as solvent.

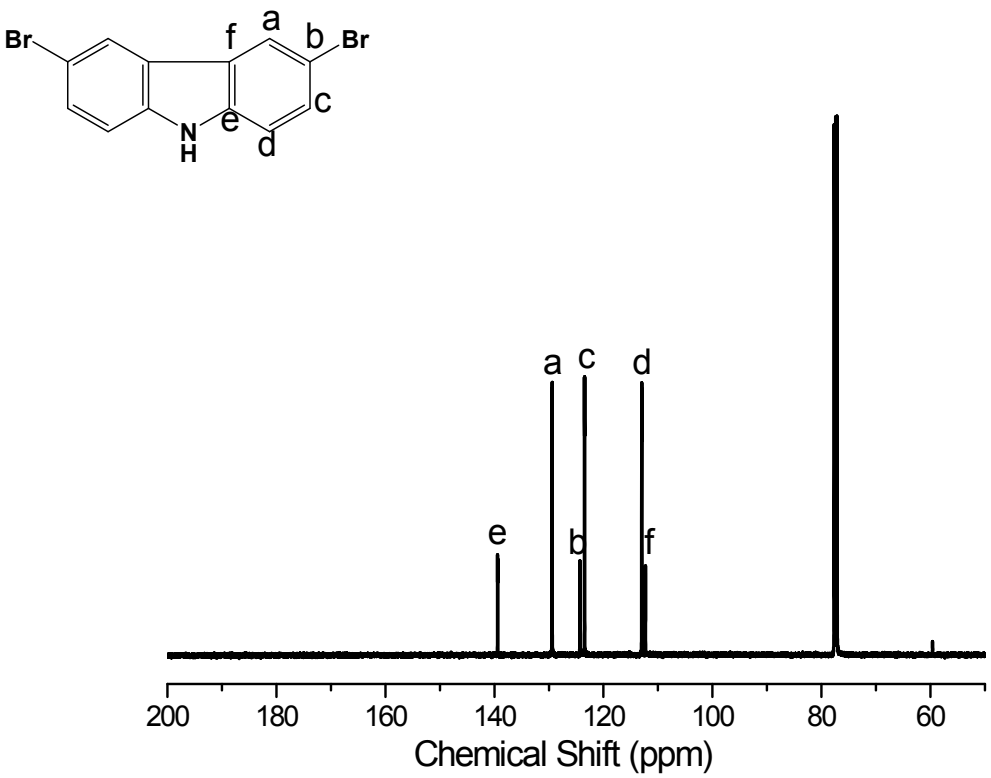

Figure S4. ^{13}C-NMR of Car-2Br in $CDCl_3$ as solvent.

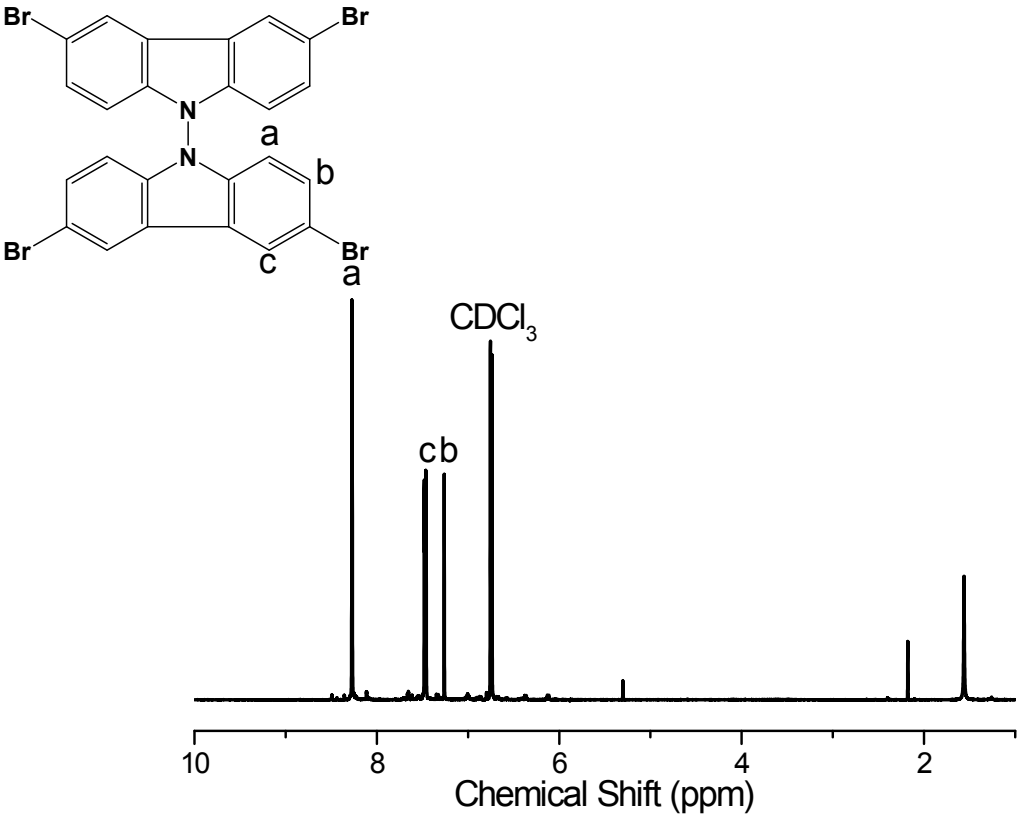

Figure S5. ^{1}H-NMR of Car-4Br in $CDCl_3$ as solvent.

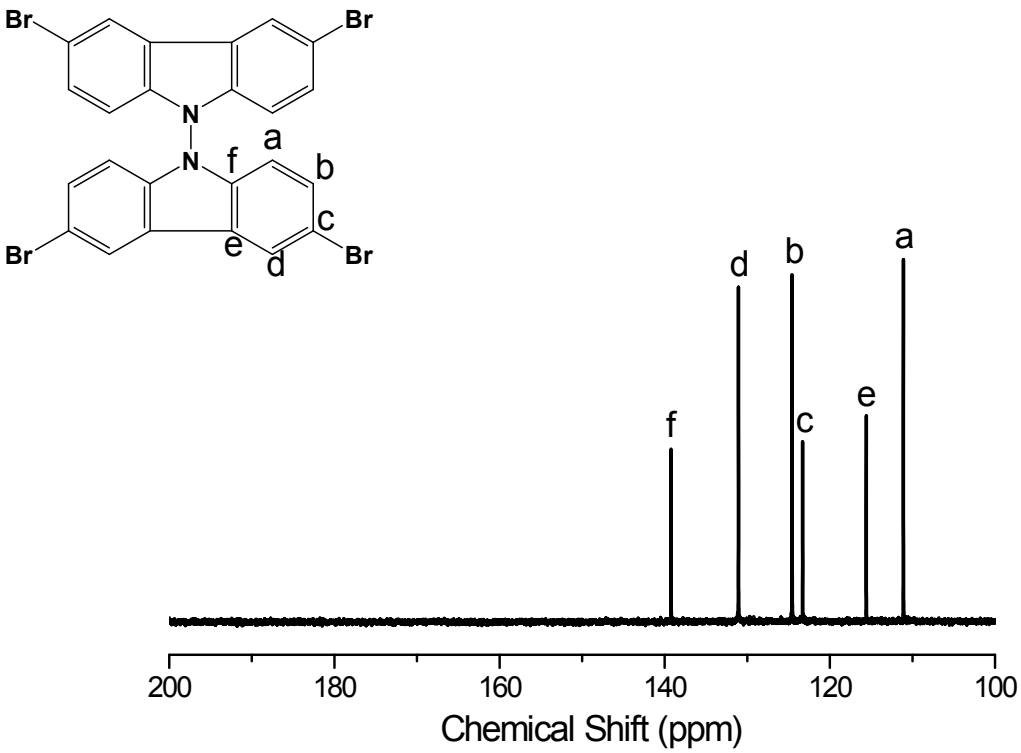

Figure S6. ^{13}C-NMR of Car-4Br in $CDCl_3$ as solvent.

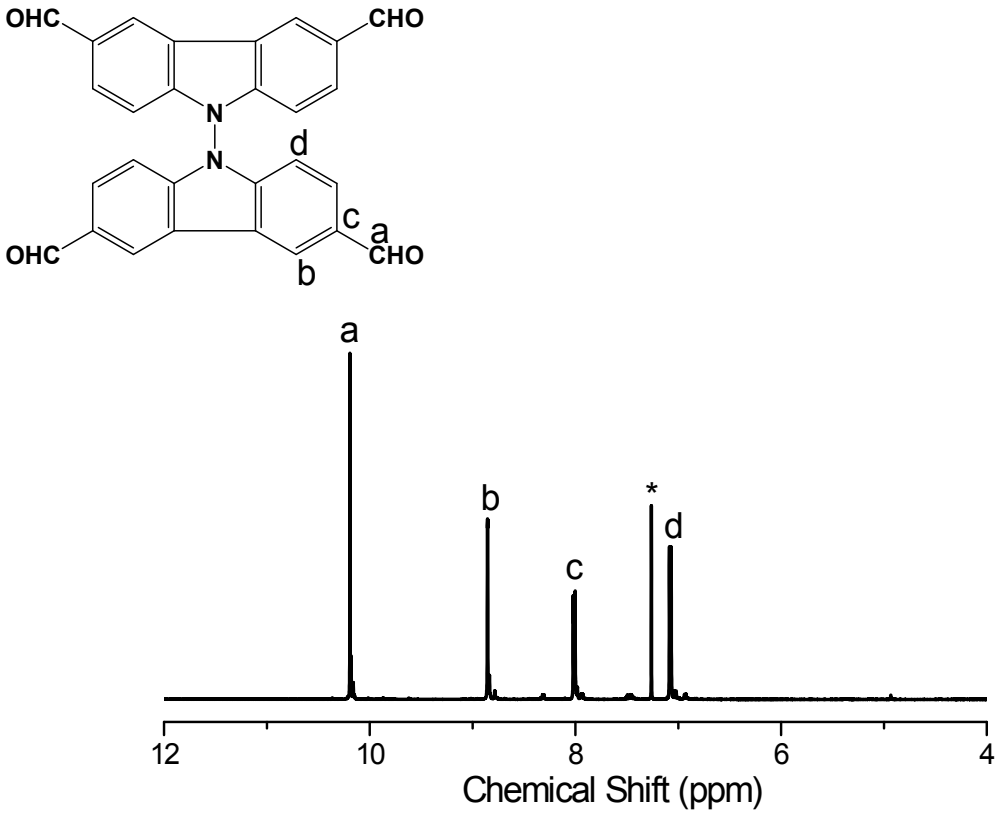

Figure S7. ^{1}H-NMR of Car-4CHO in $CDCl_3$ as solvent.

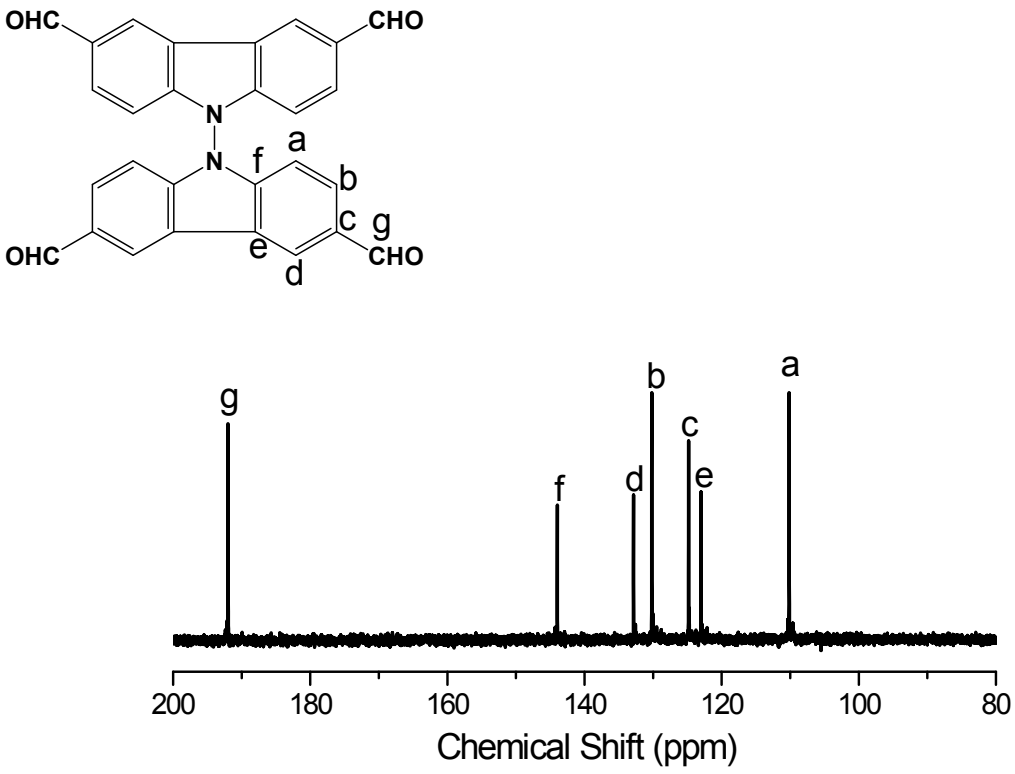

Figure S8. ^{13}C-NMR of Car-4CHO in $CDCl_3$ as solvent**.**

➢ **S4. FT-IR Spectral Profiles of Monomers and COFs**

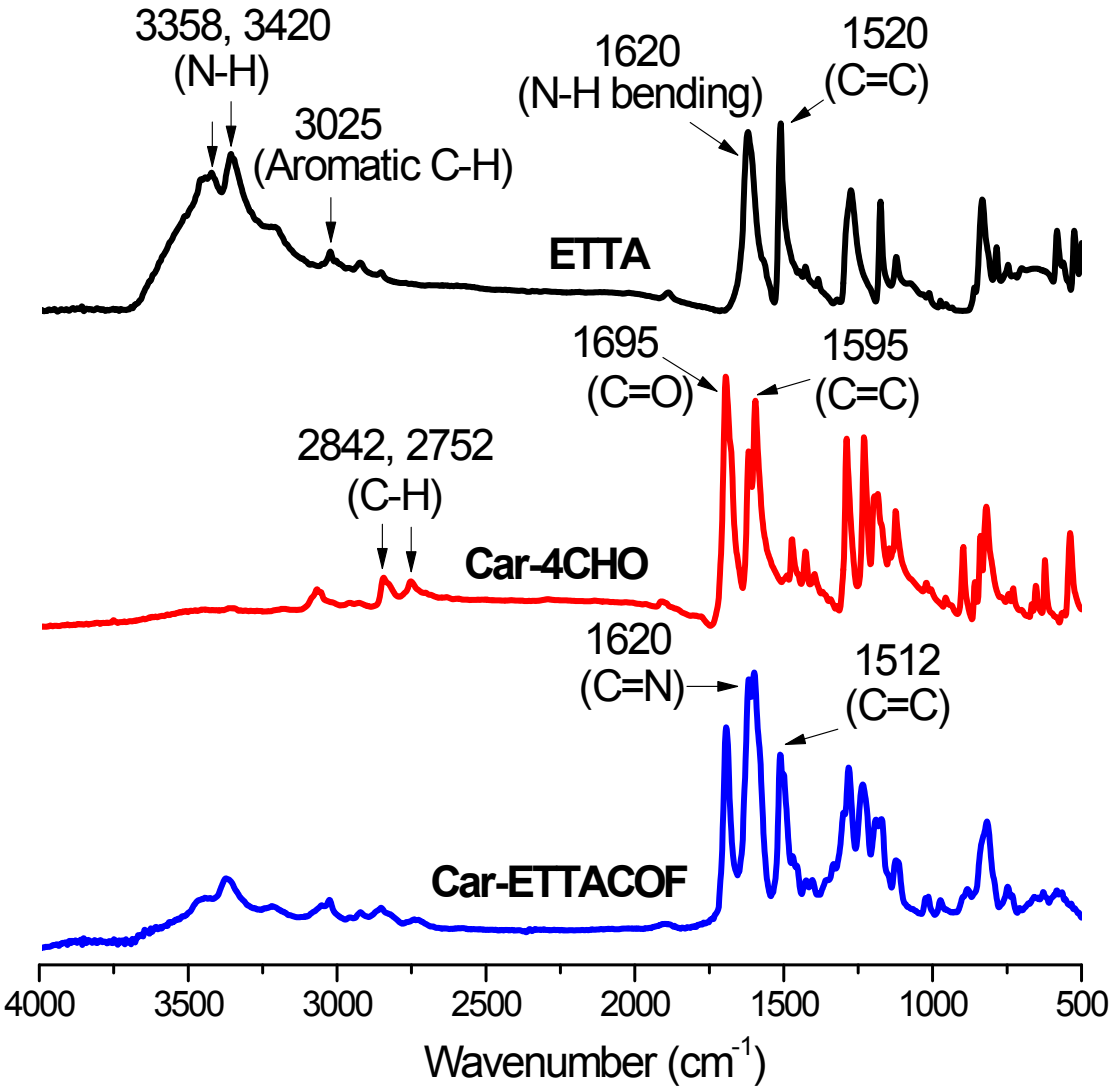

Figure S9. FT-IR spectra of ETTA, Car-4CHO, and Car-ETTA COFs.

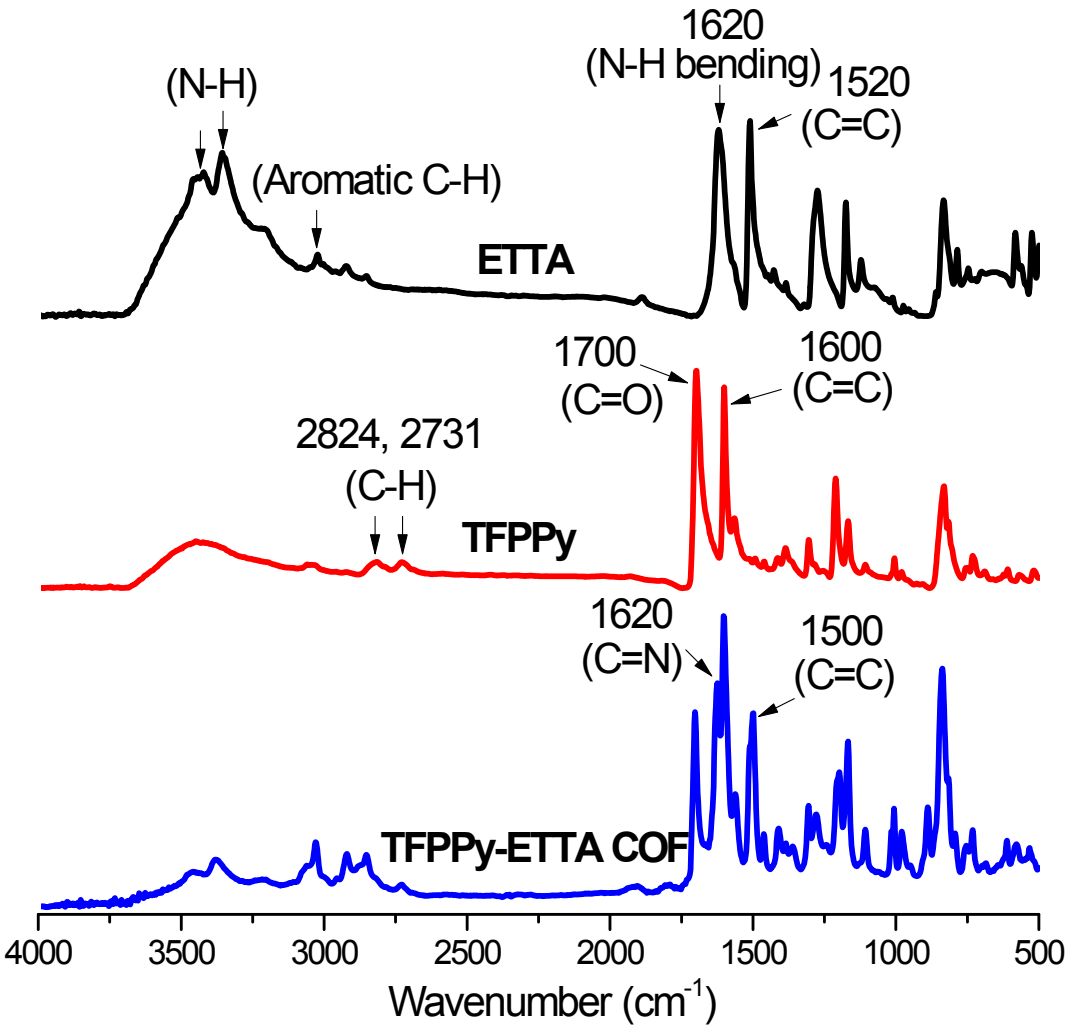

Figure S10. FT-IR spectra of ETTA, TFPPy, and TFPPy-ETTA COFs.

➢ **S5. Solid-state ^{13}C CP MAS NMR Spectra**

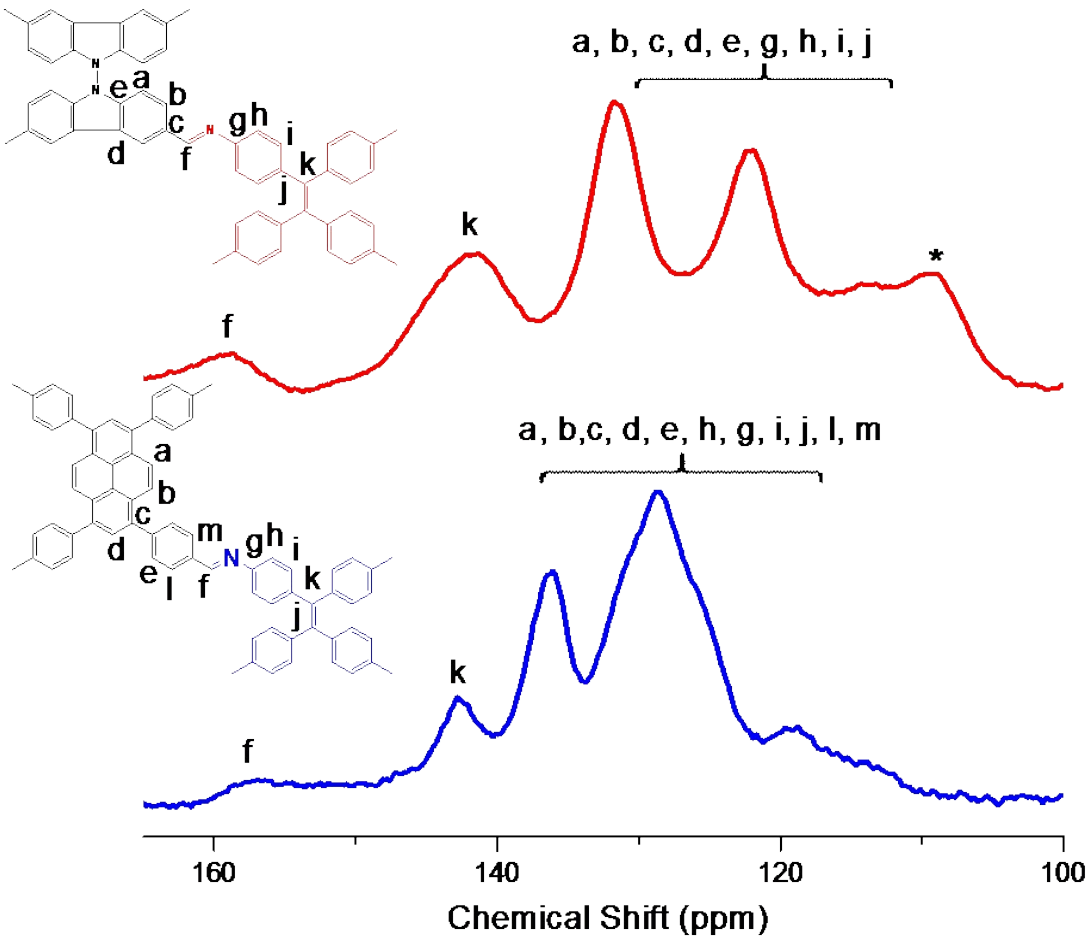

Figure S11. ^{13}C cross-polarization magic angle spinning solid-state NMR of Car-ETTA COF and TFPPy-ETTA COFs. Asterisks denote spinning sidebands.

➢ S6. Thermal Gravimetric Analysis

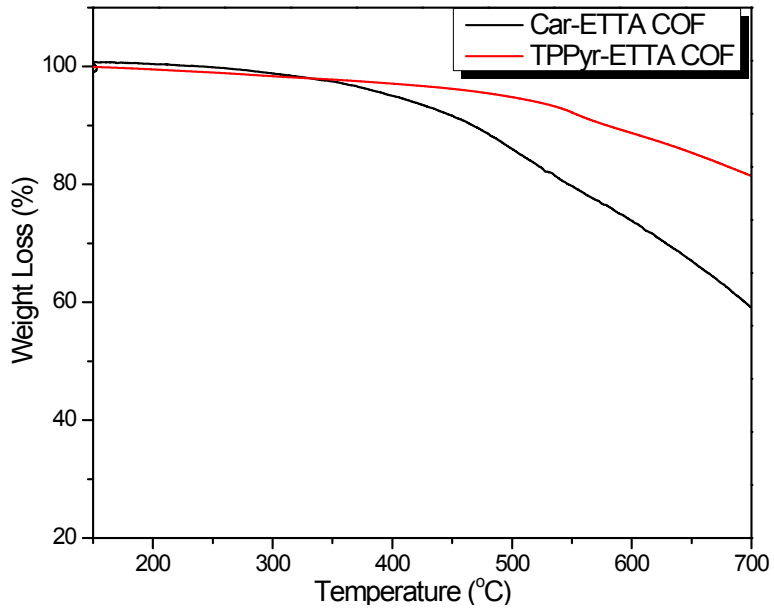

Figure S12. TGA analysis of (a) Car-ETTA COF (black line) and TFPPy-ETTA COF (red line).

Table S1. T_{d5}, T_{d10}, and Char yield of COFs.

	Car-ETTA COF	**TFPPy-ETTA COF**
T_{d5} (°C)	398	493
T_{d10} (°C)	467	580
Char yield (%)	59.3	81.5

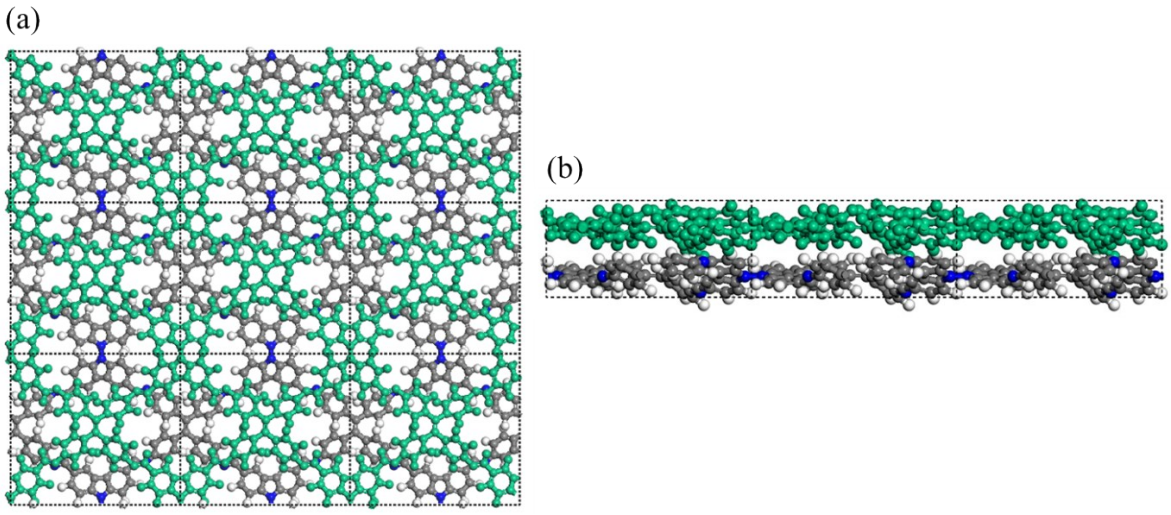

Figure S13. (a) and (b) Top and side view of the AB'-stacking model of Car-ETTA COF.

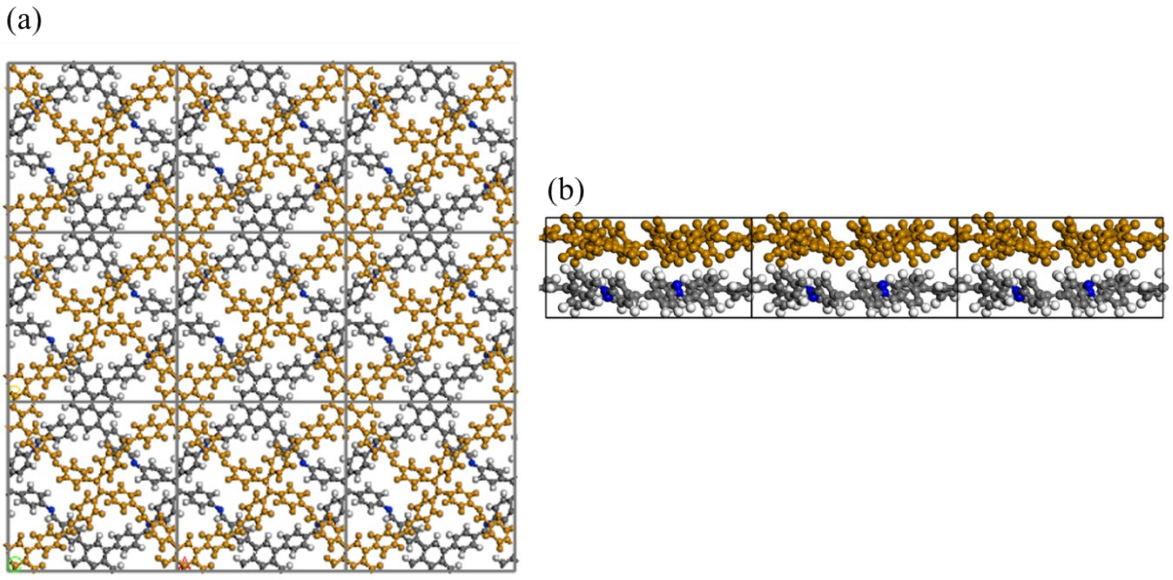

Figure S14. (a) and (b) Top and side view of the AB'-stacking model of TFPPy-ETTA COF.

Table S2. Fractional atomic coordinates for the unit cell of Car-ETTA COF.

Sample name: Car-ETTA COF							
Space group: P1 (rhombic)							
a = 19.30, b = 17.00, c = 4.60 Å, α = β = γ = 90°							
R_{wp} = 7.15%, R_p = 5.10%							
N1	0.27653	0.7269	0.48617	C20	0.14705	0.45561	0.63142
N2	0.26314	0.28516	0.43292	C21	0.66139	0.80864	0.28272
N3	0.51956	0.97588	0.55074	C22	0.67925	0.88844	0.24978
N4	0.74806	0.72136	0.47167	C23	0.63296	0.94778	0.32916
N5	0.75803	0.30852	0.68608	C24	0.56829	0.92715	0.43736
N6	0.52322	0.05917	0.58112	C25	0.54712	0.8492	0.44243
C7	0.01563	0.48098	0.53487	C26	0.59326	0.78779	0.37195
C8	0.01417	0.56316	0.50692	C27	0.46631	0.92773	0.6248
C9	0.07872	0.6121	0.47649	C28	0.40551	0.94823	0.76833
C10	0.08197	0.43123	0.52172	C29	0.35425	0.89079	0.80524
C11	0.12969	0.59395	0.27158	C30	0.36344	0.81366	0.6968
C12	0.1947	0.63141	0.2754	C31	0.4283	0.79161	0.57541
C13	0.2088	0.69046	0.47928	C32	0.47961	0.85013	0.54919
C14	0.15456	0.71553	0.66195	C33	0.71795	0.75135	0.24414
C15	0.09043	0.67672	0.66002	C34	0.30324	0.76006	0.71615
C16	0.07963	0.35493	0.39988	C35	0.9473	0.61013	0.50908
C17	0.13947	0.30884	0.36931	C36	0.94912	0.4339	0.57283
C18	0.20379	0.33595	0.46538	C37	0.93494	0.67094	0.30809
C19	0.20685	0.40939	0.60263	C38	0.8697	0.70794	0.2914

C39	0.81525	0.68435	0.47562	H63	0.16163	0.76452	0.80874
C40	0.82937	0.62904	0.69069	H64	0.05087	0.69567	0.80918
C41	0.89503	0.59471	0.71074	H65	0.03119	0.32964	0.33049
C42	0.89057	0.44645	0.39851	H66	0.13593	0.25116	0.27098
C43	0.82833	0.40667	0.44462	H67	0.25498	0.43146	0.68995
C44	0.82281	0.35013	0.66144	H68	0.15411	0.51187	0.72898
C45	0.88222	0.33219	0.82711	H69	0.73078	0.90465	0.17753
C46	0.94434	0.37416	0.78322	H70	0.64858	1.00831	0.31566
C47	0.38189	0.23941	0.45489	H71	0.57837	0.72683	0.39739
C48	0.36316	0.16299	0.35951	H72	0.39723	1.00747	0.84357
C49	0.40959	0.09975	0.38279	H73	0.30586	0.90725	0.90823
C50	0.47437	0.1132	0.50694	H74	0.43735	0.73228	0.49921
C51	0.49575	0.18893	0.57329	H75	0.7434	0.74984	0.03474
C52	0.45073	0.25345	0.55032	H76	0.27494	0.76047	0.91915
C53	0.57644	0.10231	0.69104	H77	0.97496	0.6884	0.15886
C54	0.6383	0.07481	0.80804	H78	0.86189	0.75438	0.13417
C55	0.68891	0.12905	0.8936	H79	0.78938	0.61295	0.84449
C56	0.67827	0.21048	0.85622	H80	0.90528	0.55355	0.87677
C57	0.61318	0.23823	0.7553	H81	0.8918	0.48927	0.23312
C58	0.5627	0.18215	0.68013	H82	0.784	0.41928	0.30818
C59	0.32836	0.30203	0.47547	H83	0.88133	0.28623	0.98907
C60	0.73873	0.26246	0.89645	H84	0.98911	0.36015	0.91179
H61	0.11981	0.54575	0.12888	H85	H	0.31147	0.15195
H62	0.23468	0.61326	0.12485	H86	H	0.39398	0.0416

H87	0.46697	0.31121	0.62203	H90	0.60369	0.30048	0.72676
H88	0.64834	0.01281	0.82452	H91	0.34428	0.36048	0.53937
H89	0.73819	0.10738	0.97331	H92	0.77241	0.25138	1.08003

Table S3. Fractional atomic coordinates for the unit cell of TFPPy-ETTA COF.

Sample name: TFPPy-ETTA COF							
Space group: P1 (rhombic)							
a = 21.20, b = 21.20, c = 4.5 Å, α = β = γ = 90°							
R_{wp} = 4.40%%, R_p = 3.24%							
N1	0.74486	0.63813	0.27235	C20	0.54513	0.92708	0.38660
N2	0.16636	0.72443	0.72859	C21	0.42126	0.87994	0.41406
C3	-0.01236	0.53048	0.49731	C22	0.47109	0.84058	0.33390
C4	0.02653	0.58692	0.59506	C23	0.53302	0.86260	0.32058
C5	0.07928	0.45487	0.60356	C24	0.35873	0.85117	0.44299
C6	0.06889	0.58176	0.83294	C25	0.58299	0.81547	0.24970
C7	0.11349	0.62872	0.89058	C26	0.58498	0.75788	0.40491
C8	0.11211	0.68450	0.72762	C27	0.63219	0.71353	0.34626
C9	0.06047	0.69635	0.54320	C28	0.67810	0.72577	0.12963
C10	0.01841	0.64832	0.47713	C29	0.67476	0.78211	-0.03369
C11	0.08898	0.41622	0.85123	C30	0.62694	0.82601	0.02204
C12	0.14632	0.38610	0.90153	C31	0.30861	0.87141	0.26430
C13	0.19864	0.39962	0.72253	C32	0.24924	0.84442	0.29784
C14	0.19277	0.44728	0.50933	C33	0.23992	0.79634	0.50677
C15	0.13379	0.47516	0.45170	C34	0.29044	0.77541	0.68208
C16	0.39351	1.04820	0.61606	C35	0.34965	0.80273	0.64991
C17	0.38267	0.98479	0.56008	C36	0.73170	0.68254	0.08169
C18	0.43216	0.94408	0.47840	C37	0.17892	0.76478	0.51948
C19	0.49429	0.96783	0.46456	H38	0.06654	0.54105	0.97186

H39	0.15014	0.62114	1.05414	H51	0.70921	0.79218	-0.20511
H40	0.05359	0.74176	0.4392	H52	0.62451	0.86851	-0.11072
H41	-0.01851	0.66197	0.32965	H53	0.3158	0.90783	0.09869
H42	0.05045	0.40451	0.99306	H54	0.21095	0.85995	0.15605
H43	0.14805	0.35153	1.07695	H55	0.28402	0.7378	0.84229
H44	0.23308	0.45957	0.37366	H56	0.38829	0.7868	0.7885
H45	0.13157	0.50972	0.27942	H57	0.76236	0.69253	-0.1041
H46	0.35281	1.07734	0.6594	H58	0.14785	0.77129	0.33137
H47	0.33463	0.96842	0.58046				
H48	0.46132	0.79155	0.28243				
H49	0.55119	0.74823	0.57979				
H50	0.634	0.67045	0.4755				

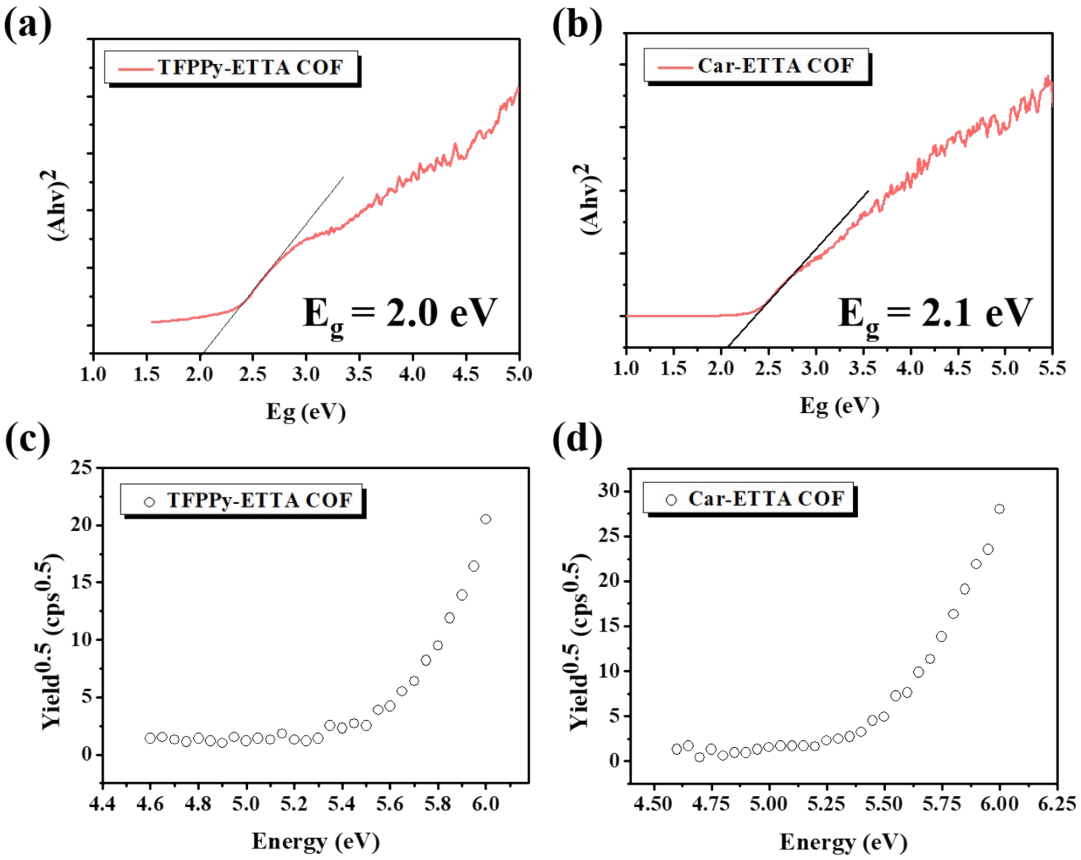

Figure S15. The Tauc plots of (a) TFPPy-ETTA and (b) Car-ETTA and the photoelectron spectrometer model of (c) TFPPy-ETTA and (d) Car-ETTA COFs.

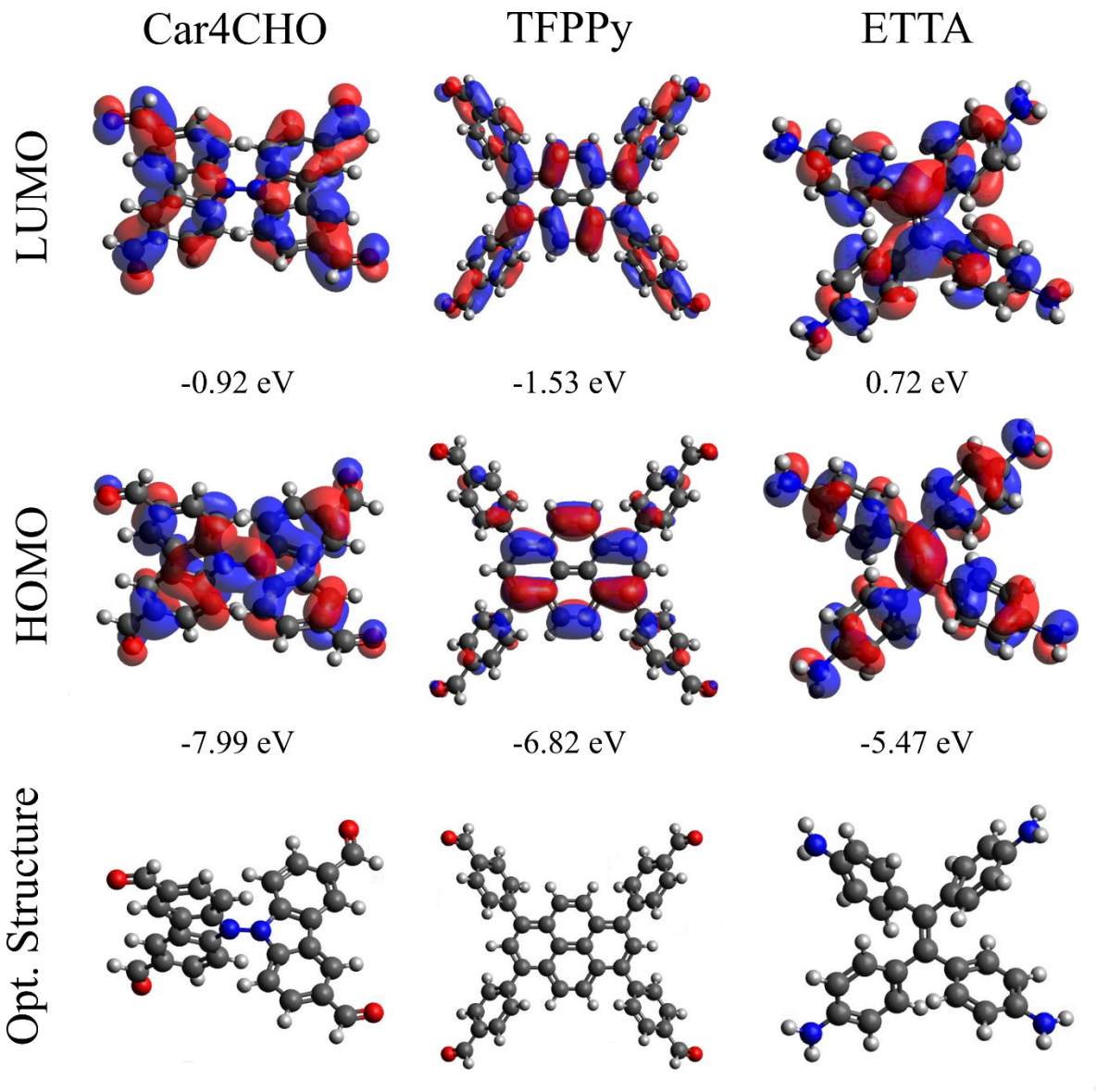

Figure S16. Optimized structure and details on the electronic frontier states of Car4CHO, TFPPy and ETTA.

Table S4. Dihedral angles in molecules, monomers and periodic structures of the Car-ETTA and TFPPy-ETTA.

	Dihedral angle (°)
ETTA	**57.3**
Car4CHO	**89.7**
TFPPy	**52.5**
Car-ETTA (monomer)	**89.2 (in Car subunit)** **13.5 (in ETTA subunit)**
Car-ETTA (monolayer)	**52.3 (in Car subunit)** **18.1 (in ETTA subunit)**
Car-ETTA (bulk)	**46.3 (in Car subunit)** **12.9 (in ETTA subunit)**
TFPPy-ETTA (monomer)	**52.2 (in TFPPy subunit)** **10.8 (in ETTA subunit)**
TFPPy-ETTA (monolayer)	**55.4 (in TFPPy subunit)** **9.4 (in ETTA subunit)**
TFPPy-ETTA (bulk)	**52.9 (in TFPPy subunit)** **7.1 (in ETTA subunit)**

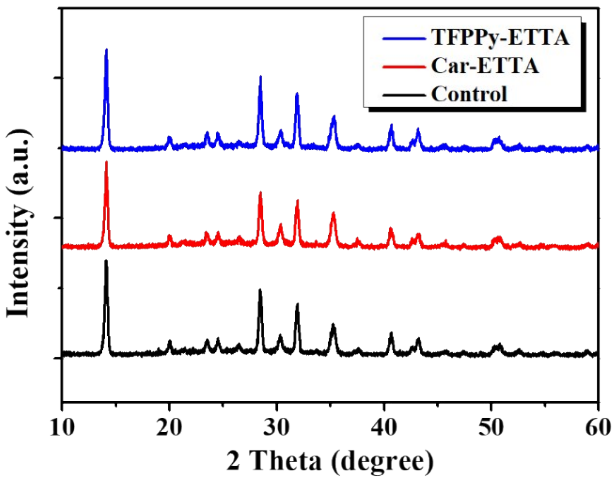

Figure S17. The XRD patterns of the perovskite film deposited on a pristine NiO_x layer and on the COF-modified NiO_x layers**.**

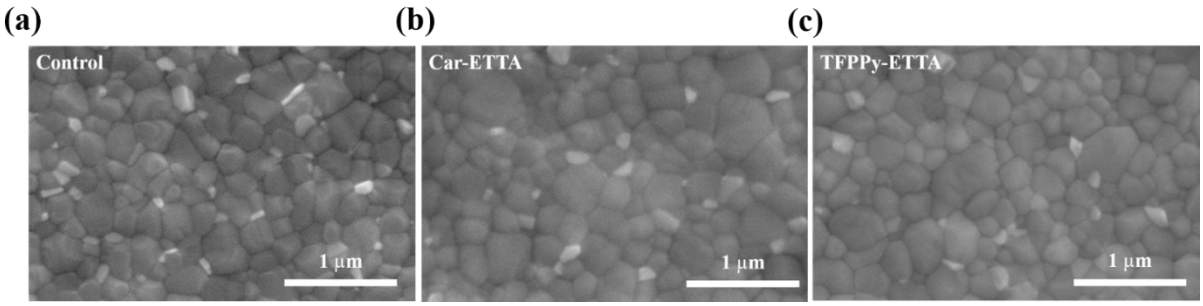

Figure S18. The SEM images of the perovskite film deposited on (a) a pristine PTAA layer and on (b, c) the COF-modified PTAA layers.

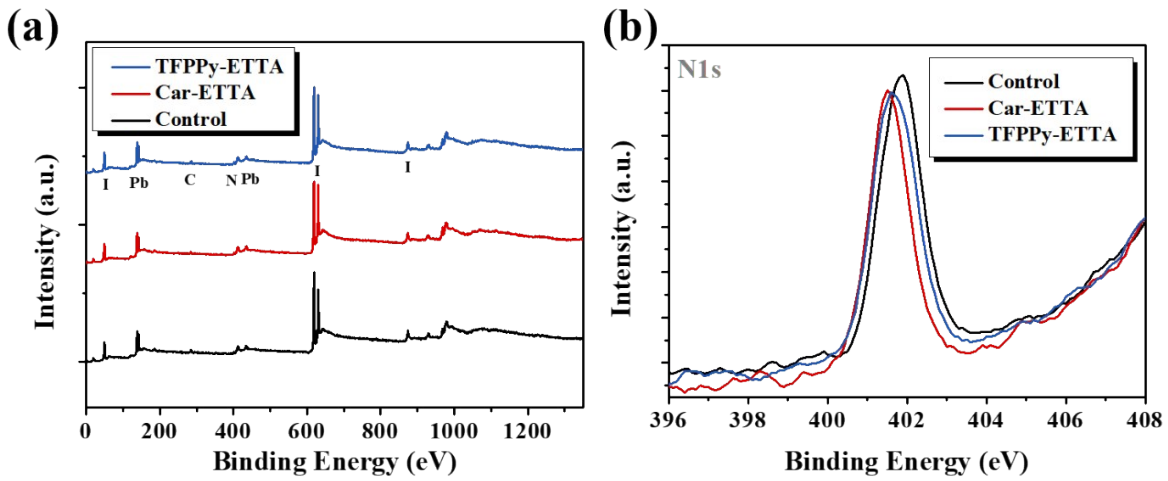

Figure S19. (a) The XPS survey and (b) N-1s spectra of studied perovskite films.

Table S5. The carrier lifetimes and related parameters of the pristine perovskite film and the films deposited on studied COFs measured by TRPL.

	τ_1 (ns)	%	τ_2 (ns)	%	τ_{avg} (ns)
Control	77.60	3.24	1478.26	96.76	1475.8
TFPPy-ETTA	58.25	6.41	972.75	93.59	969.0
Car-ETTA	184.51	28.84	580.94	71.16	535.7
PTAA	67.83	43.16	199.00	56.84	172.0
PTAA/ TFPPy-ETTA	11.24	28.25	150.98	71.75	147.0
PTAA/ Car-ETTA	18.05	47.55	135.78	52.45	123.1

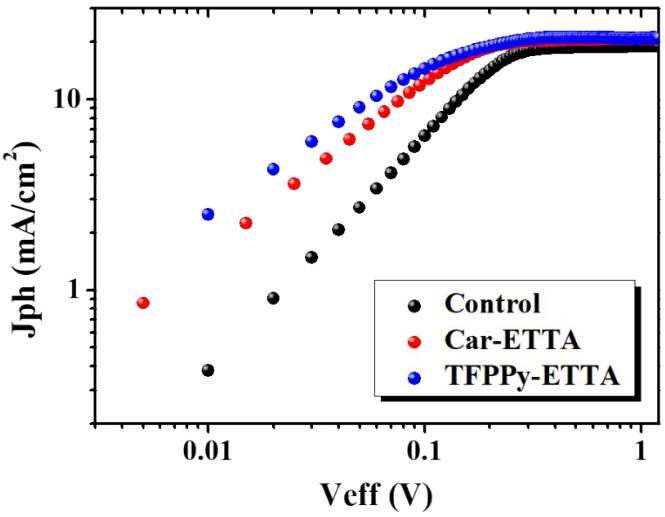

Figure S20. The J_{ph}-V_{eff} curves of the control and COF-modified devices.

References

S1. (a) P. J. Waller, Y. S. AlFaraj, C. S. Diercks, N. N. Jarenwattananon and O. M Yaghi, *J. Am. Chem. Soc*. 2018, **140**, 9099-9103. (b) M. G. Rabbani, A. K. Sekizkardes, O. M. El-Kadri, B. R. Kaafarani and H. M. El-Kaderi, *J. Mater. Chem*. 2012, **22**, 25409-25417.

S2. S. Xu; X. Bai, J. Ma, M. Xu; G. Hu; D. T. James and L, Wang. *Anal. Chem*. 2016, **88**, 157853-7857.

S3. S. Feng, H. Xu, C. Zhang, Y. Chen, J. Zeng, D. Jiang and J. X Jiang, *Chem. Commun*., 2017, **53**, 11334-11337.